STRUCTURE AND PROPERTIES MULTILAYERED MICRO- AND NANOCOMPOSITE COATINGS OF Ti-N-Al/Ti-N/Al$_2$O$_3$

A.D. Pogrebnjak[1,2], V.M. Beresnev[6], M.V.Il'yashenko[1,2], D.A. Kolesnikov[3], A.P. Shypylenko[1,2], A.Sh. Kaverina[1,2], N.K. Erdybaeva[3], V.V. Kosyak[1], P.V. Zukovski[5], F.F. Komarov[4], V.V. Grudnitskii[6].

[1]. Sumy State University, Str. R-Korsakov, 2, Sumy 40007, Ukraine
[2]. Sumy Institute for Surface Modification PO BOX 163, 40030 Sumy, Ukraine
[3]. Belgorod State University, Belgorod, Russia
[4]. Belarus State University, Minsk, Belarus
[5]. Lublin University of Technology, Lublin, Poland
[6]. Kharkov National University Kharkov, Ukraine

ABSTRACT
    This paper presents the first results on formation and studying of structure and properties of nanocomposite combined coatings. By means of the deposition processes modeling (deposition conditions, current density-discharge, plasma composition and density, voltage) we formed the three-layer nanocomposite coatings of Ti-Al-N/Ti-N/Al$_2$O$_3$/.The coating composition, structure and properties were studied using physical and nuclear-physical methods. The Rutherford proton and helium ion back scattering (RBS), Scanning Electron Microscopy with microanalysis (SEM with EDS and WDS), X-Ray diffraction (XRD) including a grazing incidence beam to 0.5°, as well as nanohardness tests (hardness) were used for analysis. Measurements of wear resistance, corrosion resistance in NaCl, HCl and H$_2$SO$_4$ solution were also performed. To test mechanical properties such characteristics of layered structures as hardness H, elastic modulus E, H^3/E^2 etc. were measured. It was demonstrated that the formed three-layer nanocomposite coatings had hardness of 32 to 36 GPa, elastic modulus of 328 ±18 to 364 ±14 GPa.
    Its wear resistance (cylinder-surface friction) increased by a factor of 17 to 25 in comparison to the substrate (stainless steel). The layers thickness was in the range of 56 – 120 μm.

INTRODUCTION
    Traditional methods of surface modification (which are: physical, chemical, electrochemical and mechanical ones [1]) as well as more advanced methods such as ion implantation, ion-assisted deposition of thin films, plasma technologies and electron beam treatment in some cases cannot result directly in a desirable way. In this connection for solving the industrial problems existing in ship building and chemistry, for instance [2], one has to combine such methods of surface modification for the production of hybrid coatings possessing the definite operation properties. An oxide-aluminum ceramics and other coatings based on titanium carbide and tungsten carbide and nitrides possess a number of useful properties, which are able to provide corrosion protection, high hardness and mechanical strength, low wear, and good electro-isolation properties [1-3].
    It is well known that Ti-Al-N nano-composite coatings feature high physical and mechanical properties such as high hardness and elastic modulus. However, high hardness values are found only in coatings with small nano-grain sizes [4].
    In ref. [4], we reported that deposition of Ti-Al-N coatings on to thick Ni-Cr-B-Si-Fe one resulted in improved physical-mechanical properties. In this case, hardness values reach only 22 ± 1.8GPa, which, first of all, was related to large nano-grain sizes of 17 to 22 and 34 to 90nm. A thin film with thickness less than 3.5μm was deposited on to Ni-Cr-B-Si-Fe thick coating of 60 to 70μm using magnetron sputtering with an alloyed Ti$_{40}$Al$_{60}$ target.

In the second paper [4,5], steel samples were coated with 2.5 µm coating by usage of vacuum-arc source in HF discharge. The fabricated coatings demonstrated high hardness reaching 35 ± 2.1 GPa combined with high wear resistance, scuffing resistance, and low friction coefficient in comparison with standard TiN.

EXPERIMENTAL

Samples of stainless steel 321 of $(2.5 \div 3)$ mm thickness were coated using plasma-detonation method by the device "Impule-6". The coating, with thickness of about 50µm, was fabricated from α-Al_2O_3 powder with 23 to 56µm grain size. Coatings were deposited within 20mm width, for one pass. Gas expenditures and battery capacity were similar to those applied in ref. [4]. After the surface purification by glow discharge, TiN coating of 1.8 to 2.2µm thickness was deposited on to Al_2O_3 coatings using 100 A arc current of Ti cathode and leaking-in N/Ar gas mixture.

Using the alloyed cathode TiAl, Ti-Al-N layers of different thickness in the range of $(2.2 \div 2.5)$ µm were deposited also in N/Ar medium. The resulting thickness of a three-layer multi-component coating reached 53 to 56.5 µm.

To analyze the coating structure, we used following methods: X-ray diffraction (XRD), TEM analysis, scanning electron microscopy with micro-analysis (SEM with EDS), and Rutherford back-scattering method (RBS) (He ions of 2.29 MeV and protons of 1.001 MeV) for composition analysis. Electron spectroscopy and corrosion tests were performed using a standard cell [4,5,6]. Wear resistance tests were performed according to the cylinder-plane scheme.

Transversal and angular cross-sections $(7 \div 10°$ angle) were prepared for several samples to analyze depth element distribution over the total multi-layered coating. They were used for electron microscopy, micro-analysis, point-by-point XRD-analysis, and nano-indentation.

To investigate the homogeneity of powder coatings and identify the various inclusions of the matrix substrate in the contact area for 10 minutes. The surface was etching using solution of hydrofluoric acid (50 ml HF, 50 ml H_2O). The structure of the steel studied in the transition region was determined after subsequent grinding and etching (t = 10 min.) Nitric acid solution (2 mL HNO_3, 48 mL ethyl alcohol).

The elemental distribution in the coatings, before and after corrosion treatment, was evaluated by the Rutherford Back-scattering Spectroscopy (RBS) at the 5.5 MVTandemAccelerator of the NCSR DEMOKRITOS/Athens using a deuteron beam of 1.5 MeV energy (scattering angle: 170°, solid angle: $2.54 \times 10^{"3}$ sr). Nuclear reaction analysis using the same accelerator was used for the determination of the N depth distribution on the samples ($^{14}N(d, a)^{12}C$ nuclear reaction, Ed =1.350 MeV, detector angle: 150°, detector solid angle: $2.54 \times 10^{"}3$ sr) .

For the RBS and NRA measurements a C. Evans & Assoc. scattering chamber equipped with a computer controlled precision goniometer and a laser positioning system was utilized. The vacuum in the scattering chamber was constant (ca. 2×10^{-7} Torr). The beam current on the target did not exceed 10 nA, while the beam spot size was 1.5 mm×1.5 mm.

The analysis of the NRA and RBS data was performed using the simulation code RUMP [7].

The corrosion resistance of the prepared coatings was investigated using electrochemical techniques. An AUTOLAB Potentio-Galvanostat (ECO CHEMIE, Netherlands) and Princeton Applied Research corrosion testing cell were used for the electrochemical measurements. A saturated calomel electrode used as a reference electrode and a graphite one as an auxiliary electrode for all measurements.

The tests in 0.5 M H_2SO_4 solution were carried out in the potential region −1000 to +1500 mV at ambient temperature. Five rapid scans (scan rate=25 mV/s) followed by one slow scan (scan rate=0.25 mV/s) were performed on each specimen. The rapid scans allow investigations under constant conditions of the material surface and corroding medium, whereas slow scans lead to predictions of the general corrosion behavior of the material. In all cases the sample surface exposed to

the corroding medium was 1 cm^2 [5-7]. The above-mentioned experimental conditions were also applied for the corrosion tests in HCl and NaCl solutions, whereas the scanning region was from −300 to +1700 and from −1000 to +1000 mV, respectively [5].

RESULTS AND DISCUSSION

Table 1 presents the results of calculation for nano-hardness and elastic modulus for every layer of the multi-layered system. One can see that nano-structured Ti-Al-N featured the highest hardness of 35 ± 1.8 GPa and the highest elastic modulus 327 ± 17 GPa. Evaluations of grain sizes performed according to Debay-Sherer method, demonstrated that grain size in near surface layer was in the range of 10 to 12 nm, at the same time, the second TiN layer demonstrated sizes of 30 to 35nm and Al_2O_3 coating demonstrated wide variation of values from units of a micron (5% of grains) to tens of micron (25%) and grains exceeding 100nm (less than 20%). Thus, the third layer of Al_2O_3 ceramics turned out to be dispersion-hardened rather than nano-structured one.

Table 1. The values of hardness and modulus of elasticity, the size of layers sandwich of nanocomposites combined coatings deposited on stainless steel

Composition of coating (layer)	H, GPa	E, GPa	Grain size (nm)	Thickness of layers (μm)
Ti-Al-N	35±1,8	327±13	10–12	2,2–2,5
Ti-N	22±6	240±16	20–35	1,8±0,2
Al_2O_3	16 – 20	194±8	10^4–10^5	48–52
Steel	4,2	46±2,5	10^5–10^6	$2 \cdot 10^3$

Figure 1 shows an image of a transversal cross-section of a thin Ti-Al-N coating and that of a thick one Ni-Cr-B-Si-Fe . An EDS microanalysis was performed over the cut section, and the results are presented in Fig.2a, b, c. The presented spectra indicate that in the thin coating only titanium and aluminum were present.. The interface of the thin film and the coating contained Ti, Al, N,Ni, Cr, Fe, and Si at some places. In the thick coating we found Ni, Cr, Fe, Si, Ni amounting 45%, and all the rest was the mentioned above elements.
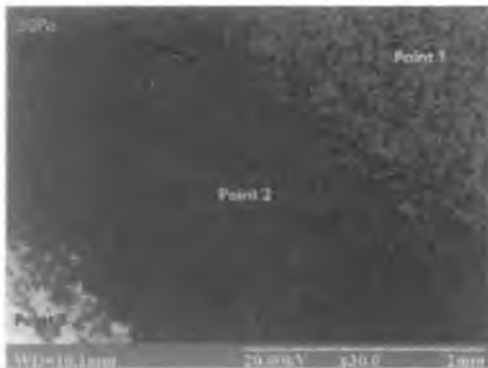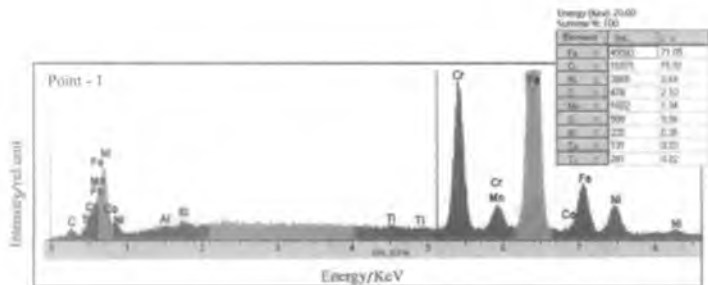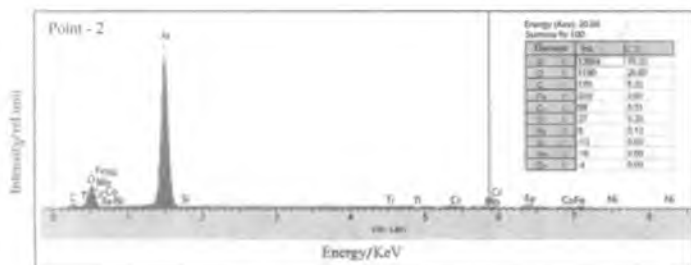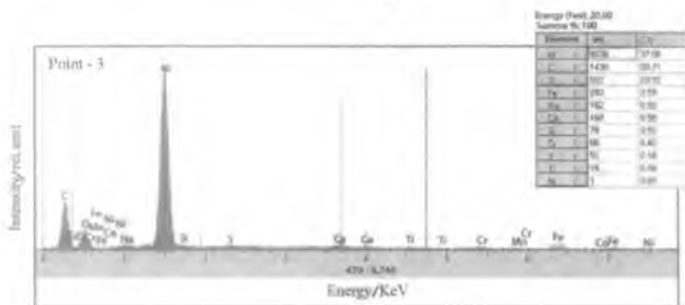

Fig.1 The image of coating cross-section prepared at an angle 7-10° multilayer nanocomposite coatings based on Ti-Al-N/Ni-Cr-B-Si-Fe.

Fig.2 – The Energy-dispersive spectra obtained from the "angle lap" sections of multilayer surface beginning from the interfacial area of the Al₂O₃ coating (substrate (a), the second layer (b), third (the top layer (a)) shown in Figure 1.

Figure 3 shows the RBS spectra of He ions (a) and protons (b). In this coating, Ni, O, Al, Ti elements and small concentration of Nb atoms, as well as very small amount of Ta were observed. The latter came from chamber walls as non-controlled impurity. When the spectrum formed a step, the compound stiochiometry, which was obtained from RBS spectra according to formulas [6] demonstrated $Ti_{60}Al_{40}$ values. The used proton beam energy was sufficient to analyze the second layer of TiN over its depth and the next one of Al_2O_3 including the interface of Al_2O_3 layer (relative to the substrate). The analyzing proton beam could not reach the back Al_2O_3 interface because of insufficient energy. The images of coating cross-sections showed three layers of different thickness.
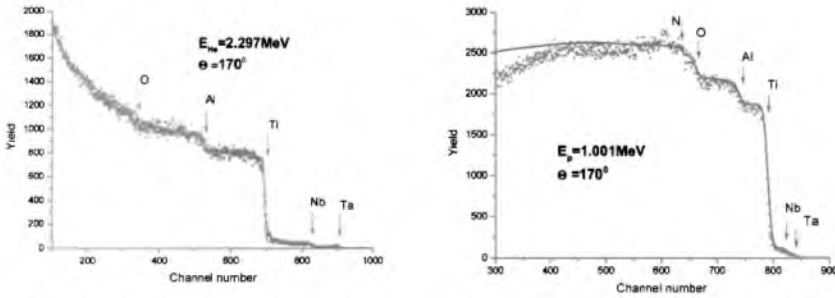

Fig.3. RBS experimental spectra obtained for multi-layered $Ti-Al-N/Ti-N/Al_2O_3$ coating. Helium ion energy was 2.297MeV (a) and proton energy was 1.01MeV (b).

Visual analysis indicated good quality of the obtained coatings, which did not include pores but exhibited surface roughness resulting from the plasma-detonation treatment. All subsequent layers repeated this roughness, diminishing it a little degree due to smoothed interfaces between protuberances and valleys. However, after deposition of the thick Al_2O_3 we polished surface was carried out on the grinding machine with diamond paste. for RBS measurements. The cross-sections were prepared for micro-analysis and nano-indentation tests. Point-by-point micro-analysis, which was performed in angular cross-section starting from the substrate, demonstrated that the first layer was composed of Ti-Al-N, the second one – of TiN, and the third one of Al_2O_3.

Figure 4 shows diffraction patterns for multi-layered nano-composite coatings of Ti-Al-N/Ti-N/Al_2O_3 at the initial state. As it is seen in this Figure, Al_2O_3, TiN, $AlTi_3N$, (AlTi)N phases are presented in this coating. $Cr_{0.19} Fe_{0.7} Ni_{0.11}$ phase, which came from the substrate, was also possible.

After 600°C annealing, the coating phase composition was changed. However, 900°C annealing during 3 hours in air (the diffraction pattern in Fig.4, the upper curve) resulted in formation of TiO_2 and phase of Al_2O_3 became more micro-crystalline and contained only α-Al_2O_3, i.e. total oxidation of Ti and Al occurred as a result of 900°C annealing in air. Coating hardness also decreased from 14.8 GPa to 8.8 – 12 GPa. In such a way, the upper two layers were oxidized (probably the first one totally and the second one partially). The layer, which was composed of Al_2O_3, did not demonstrate transition from γ-phase to α-one, possibly because it starts at temperatures higher than 900°C.
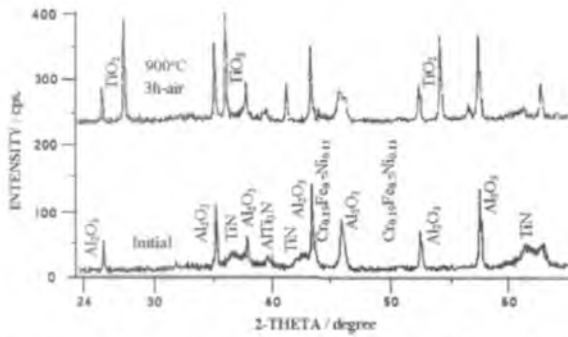
Fig.4. Diffraction patterns for multi-layered nano-composite Al-N/Ti-N/Al$_2$O$_3$ coating after deposition (in several weeks) and after 900°C annealing in air during 3 hours.

Auger-electron microscopy, which was performed for these coatings, demonstrated Ti, N, Al, O, and C elements. At the initial moment of deposition, the concentration of these elements was changed, but after the etching during more than 12 min, their profile did not change. Additional studies performed using nuclear reactions method, allowed us to obtain depth element profiles for two upper layers including the interface between the second and the third layer. Thickness of Ti-Al-N and Ti-N layers was accurately measured. It amounts to 4.27μm. Measurements after 900°C annealing of the multi-layered systemdemonstrated essential changes of element concentration profiles over depth. The upper layer was enriched with oxygen and carbon, that indicated formation of Ti and Al oxides. This was confirmed by XRD analysis.
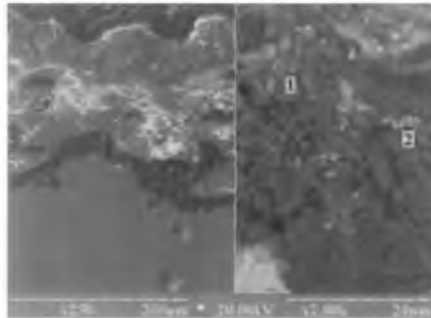

Fig.5. (a) and (b) show images for coating surfaces before and after annealing in air at 600°C, and for etched angular cross-sections. These images demonstrated no essential changes in the coating structure and element composition.

Fig.5. Structure of transversal cross-section in multi-layered nano-micro-composite coating (left) and surface image (right) in the initial state after deposition (in three months).

Measurements of lattice parameters for TiN, (Ti, Al)N, and Al$_2$O$_3$ coatings demonstrated that 600°C annealing decreased stresses arising in lattices: both macro-stresses at film-film and film-thick coating interfaces and micro-stresses arising in nano- and micro-grain structures.

Figure 6 a, shows the concentration profiles of the depth distribution of titanium atoms in hybrid coatings. According to the results the minimum concentration of titanium atoms in the surface region has coatings in the initial state. The maximum concentration of titanium atoms (about 52 at.%) was observed at the distance of 1.4 μm from the surface.

High concentrations of oxygen and aluminum were found in the subsurface area of titanium nitride. Depending on the mode of electron-beam melting of metal-ceramics underlayer the percentage and the depth distribution of elements changes (Fig. 6 b, c, d). For example, in the surface of the hybrid coatings after electron-beam exposure with the power density of 360 W/cm^2 in plasma-detonation sublayer of aluminum oxide in the titanium nitride film, aluminum atoms are missing.
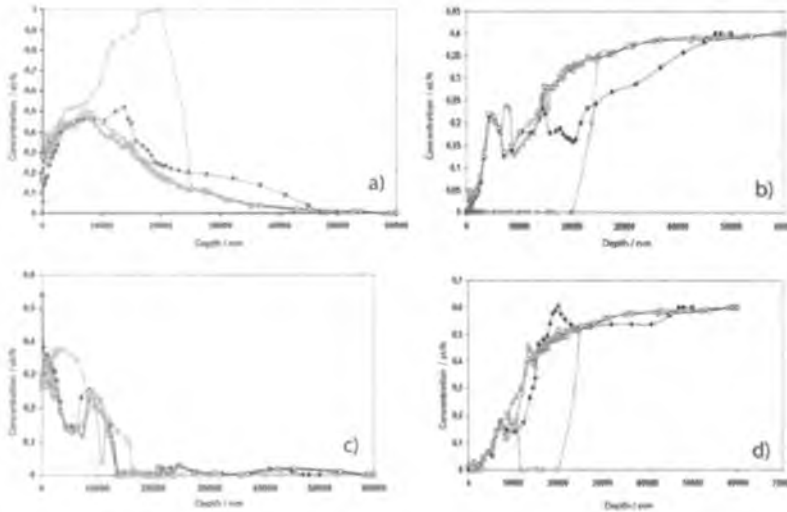

Fig.6 - The depth distribution of the constituent elements of the hybrid coatings surface: a)– Ti; b – N; c) – Al; d) – O (← without electron-beam melting; ◻ - 240 W/cm^2; △ - 300 W/cm^2; ⊖ - 360 W/cm^2).

Figure 7 shows results of wear tests, which were performed according to the plane-cylinder scheme. These results demonstrated that the most essential wear occurred in the substrate surface (curve 1). After deposition of Al$_2$O$_3$ coating by plasma-detonation technology (curve 2) wear sharply decreased. In the case of TiN deposition, wear was lower than in the case of Al$_2$O$_3$ (curve 3). The lowest wear was found in the case of multi-layered coating Ti-Al-N/Ti-N/Al$_2$O$_3$ (curve 4) [5-7].

Corrosion tests performed in Electro-Chemical Lab (Thessaloniki, Greece) using International standards in 0.5 M H$_2$SO$_4$ solution and by simple micro-weighing after definite time period (3 to 6 months) in NaCl and HCl solutions, demonstrated high coating resistance in comparison with that of stainless steel 321 substrate (European standards).
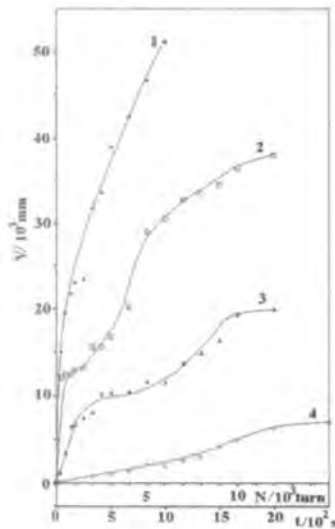
Fig.7. Dependences of material wear tested by cylinder friction over the sample surfaces: 1 – initial state; 2 – Al_2O_3 coating; 3 – TiN/Al_2O_3 coating; 4 – multi-layered nano-micro-composite coating of Al-N/Ti-N/Al_2O_3.

CONCLUSION

The fabricated multi-layered nano-micro-composite coatings based on Ti-Al-N-Ti-N/Al_2O_3 system featured thermal stability in air till 900° C. They also featured high wear resistance under cylinder friction over their surfaces and high corrosion resistance in NaCl and H_2SO_4 medium. However, 900° C annealing resulted in total oxidation of the upper Ti-Al-N layer and partial oxidation of Ti-N one. The coating hardness decreased more than by factor of 2. At the same time, electron pulsed beam (without melting) did not decrease surface hardness, possibly, due to its short-time action. However, it results in redistribution of impurities (coating components) at interfaces of this multi-layered coating.

REFERENCES

[1]J. Musil, H. Hruby, Superhard nanocomposite $Ti_{1-x}Al_xN$ films prepared by magnetron, *Thin* Solid *Films*, **365**, 104-109 (2000)

[2]Zhu J. Ye L. Li Wang F., Fabrication of TiN/Al_2O_3 Composites by a Novel Method, *Appl. Mech. and Mater.* **44-47**, 2504-2508 (2011)

[3]P. Budzynski, J. Sielanko, Z. Surowiec and P. Tarkowski, Properties of (Ti,Cr)N and (Al,Cr)N thin films prepared by ion beam assisted deposition, *Vacuum.* **83**. S186-S189 (2009)

[4]A.D.Pogrebnjak, A.A.Drobyshevskaia, V.M.Beresnev, M.K.Kylyshkanov, G.V.Kirik, S.N.Dub, F.F.Komarov, A.P.Shypylenko, Yu.Zh.Tuleushev, *Jour.Tech.Phys,* **81**, (2011).

[5]V.M. Beresenev, A.D. Pogrebnyak, P.V. Turbin, S.N. Dub, G.V. Kirik, M.K. Kylyshkanov, O.M. Shvets, V.I. Gritsenko and A.P. Shipilenko, Tribotechnical and Mechanical Properties of Ti-Al-N Nanocomposite Coatings Deposited by the Ion-Plasma Method, *Journal of Friction and Wear*, **31**, №5, 349-355 (2010).

[6]A.D. Pogrebnjak, Yu.A. Kravchenko, S.B. Kislitsyn, Sh.M. Ruzimov, F. Nolid, P. Misaelides and A. Hatzidimitriou, $TiN/Cr/Al_2O_3$ and TiN/Al_2O_3 hybrid coatings structure features and properties resulting from combined treatment, *Surface and Coatings Technology*, **7**, 2621-2632 (2006).

[7]A.D. Pogrebnjak, M.M. Danilenok, A.A. Drobyshevskaia, V.M. Beresnev and N.K. Erdybaeva, et.al. Investigation of the structure and physicochemical properties of combined nanocomposite coatings based on Ti–N–Cr/Ni–Cr–B–Si–Fe, *Russian Physics Journal*, **52**, 1317 – 1324 (2009)

[8]Pogrebnjak A.D., Shpak A.P., Azarenkov N.A., Beresnev V.M. Structures and Properties of Hard and Superhard Nanocomposite Coatings//Usp. Phys. **179**(1), 35-64. (2009)